



Thermodynamic and economic analysis of reverse osmosis and multi-effect thermal vapor compression desalination systems: a comparative study

Ziyin Liu^{a,*}, Shijun Zhang^b, Zofia J. Kilburn^c

^aCollege of Management, Queen Mary University of London, London, UK, email: Lzy475996954@163.com

^bHenan Polytechnic University, Personnel Division, Henan Jiaozuo, 454002, China, email: Zhangshoww@gmail.com

^cDepartment of Mechanical and Industrial Engineering, Tallinn University of Technology, Ehitajate tee 512616 Tallinn, Estonia, email: zofiajkilburn@gmail.com

Received 15 April 2020; Accepted 8 December 2020

ABSTRACT

Several regions are confronting a severe scarcity of freshwater due to the gap between supply and demand specially in arid and semi-arid regions. To address freshwater crisis, the present study focuses on a comparative analysis of two well-known desalination systems including reverse osmosis (RO) and multi-effect desalination thermal vapor compression (MED-TVC) from the thermodynamic and thermoeconomic viewpoints. Technical analysis of both desalination units is performed based on mass and energy balance equations. Besides, the economic study is conducted using total annual costs. Optimization of both systems to minimize the levelized cost of the product for producing 3,000 m³/d potable water is presented using particle swarm optimizer. A parametric study is also carried out to analyze the effect of key parameters on the performance criteria. Effect of parameters such as last effect temperature, heating steam temperature, motive steam pressure, and temperature difference of effects on water production and initial cost in MED-TVC process and the effect of feed water pressure, number of pressure vessels, and membrane numbers in RO unit on recovery rate and the total cost was investigated. The results show that the payback time is 3.86 and 7.76 y for optimized RO and MED-TVC units.

Keywords: Desalination; Reverse osmosis; MED-TVC; Technoeconomic analysis; Optimization

1. Introduction

With the increment of the world population and the development of living standards, potable water requirements have augmented considerably. The freshwater scarcity has become an urgent issue that can disrupt the nation's social and economic growth in the long term [1]. Water desalination processes are a great solution to overcome the problems of freshwater insufficiency existing worldwide, especially in Middle Eastern countries [2]. The leading technologies of water desalination are thermal and membrane methods, which are further classified into subgroups.

Thermal processes including multi-effect desalination thermal vapor compression (MED-TVC), multi-effect distillation (MED), and multi-stage flash (MSF). On the other hand, membrane processes are mainly reverse osmosis (RO) and electro dialysis (ED) [3,4]. Thermal desalination processes, especially the combination of the desalination plants and power generation cycles, possess a considerable share of the global desalination market. In the Persian Gulf region, thermal processes account for 70% of the desalination industry [5]. On the other hand, the RO desalination process was introduced in the 1970s to desalinate the seawater and brackish water, which has been recognized as one of the

* Corresponding author.

most advantageous methods of potable water production in the desalination industry [6]. RO is a kind of high-pressure filtration process in which a semi-permeable membrane is used to permit the water to pass through, but the salt particles are not allowed to pass through the membrane [7].

Heretofore, various thermal seawater desalination methods, including MED and MSF methods, have been presented in the different literature to produce potable water and required water for industrial sections. Since the oil is abundant in the GCC (Persian Gulf Countries) countries as well as the MENA (the Middle East and North Africa) areas, thermal seawater desalination plants are interested in such regions [8]. At present, around 41% of the whole desalination market belong to GCC regions, and from this amount, about 56% is provided by the thermally driven desalination approaches [9]. Based on the UPR (universal-performance-ratio) factor as a novel suggested criterion, the MED methods' efficiency is higher in comparison with the MSF. This criterion is defined as the evaporative energy and the initial energy ratio. This factor's value is obtained 60 and 88 for MSF and MED methods [10,11]. The system's efficiency can be enhanced by the combination of the MED/MSF with the RO method, and the total recovery will be controllable through the operating temperature of the MED/MSF [12]. Also, the MED system combination with the AD (adsorption desalination) system can double the water production compared with the traditional MED cycles [13–15].

A precise model may result in selecting the most appropriate elements and optimum operational circumstances for the promotion of the desalination systems' efficiency, decreasing energy utilization rate, and reducing expenses. In this regard, various investigations are performed based on the first and second laws of thermodynamic. In the thermal desalination plants, energy analysis is necessary to assess the system; however, the quality of the transferred energy is not regarded in the energy analysis, and this analysis cannot depict the location of the highest losses of the available energy. In contrast, the exergy analysis can detect the position, reasons, and energy depreciation levels of the system [16]. The before-mentioned data can be utilized to determine which elements can enhance the total exergy performance and optimization of the designing process [17]. For instance, Han et al. [18] used experimental analyses to evaluate the exergy approach to enhance the entrainment efficiency of the TVC by the entrained vapor preheating. The combined MED-TVC plant is optimized thermally and economically to minimize the generation costs by Sayyaadi and Saffari [19]. Also, Sharaf et al. [20] suggested a mathematical and economical formulation to model the MED-TVC system driven by a photovoltaic thermal system. An analysis is performed by Esfahani et al. [21] from the exergy perspective. They employed a GA (genetic algorithm) based multi-objective algorithm combined with an artificial neural network (ANN) to optimize a MED-TVC desalination plant.

A comprehensive thermodynamic analysis from energy and exergy perspective was carried out by Sadri et al. [22]. They resulted that the rate of exergy destruction for the RO subsystem is lesser than the MED subsystem. They also executed a multi-objective optimization regarding the first and second laws efficiencies as the cost function to obtain the optimal solution. The multi-objective optimization result

exhibited the optimum values for the energy and exergy efficiencies of 8.63% and 12.84%, respectively. Qureshi and Zubair [23] studied the effect of some significant parameters including isentropic efficiency of pump and turbine, salinity, and mass ratio on the exergy efficiency of the RO desalination system. The results exposed that an increase in pump isentropic efficiency from 75% to 85% leads to enhancing the exergy efficiency by approximately 5%. Besides, they revealed that the rise in the mass ratio from 1 to 10, increase the exergy efficiency by about 7.5%. Lee et al. [24] conducted a dynamic study of an industrial RO system using Aspen software. El-Emam and Dincer [25] studied the RO system from the energy, exergy and exergoeconomic viewpoints in various salinities. They showed that for the salinity value of 35,000 ppm, the exergy efficiency is obtained at 5.82% with a total product cost of 2.451 \$/m³.

The MED-TVC desalination unit's application among the thermal processes and the RO desalination system amongst membrane processes have increased in recent years. Therefore, a comprehensive study of these two desalination methods in the same conditions is essential for potable water production. Ortega-Delgado et al. [26] performed a thermoeconomic analysis of the cogeneration of electricity and water based on parabolic trough mirrors and direct steam generation. The location considered for this plant is Almeria, in the southeast of Spain. Two different seawater technologies have been selected to be coupled with the solar thermal power plant: multi-effect distillation and RO. Based on the obtained results, the seawater reverse osmosis (SWRO) desalination unit provides freshwater at the lower cost. It has been shown that decoupling the SWRO plant from the power plant is found as the best configuration, reaching the levelized water cost a value of 0.76 €/m³, against the 1.055 €/m³ in the RO1 case. The MED1 and MED2 configurations provide 1.239 and 1.265 €/m³, respectively, being significantly higher than the RO cases. In another work Ortega-Delgado et al. [27] carried out a comprehensive exergy analysis of a RED-MED HE (reverse electro dialysis-MED heat engine). According to their obtained results, the multi-effect distillation unit is responsible for the highest exergy destruction rate followed by the RED unit. Shakib et al. [28] analyzed a hybrid desalination system composed of multi-effect desalination with thermal vapor compression and RO plants. They concluded that despite the scenario under consideration, configuration 1 (the exit water of the cooling system in MED-TVC has been applied for the RO unit) has the minimum energy consumption and maximum exergy efficiency.

1.1. Main novelties and contributions

Based on the literature survey presented above, comparative analysis of the MED-TVC and RO systems has not presented in the present form yet. Thus, in the present study, a comparative study of two well-known desalination systems (MED-TVC and RO) to produce a certain amount of freshwater with the same salinity is presented from the economic viewpoint. Also, in this paper, optimization through particle swarm optimizer (PSO) aims to minimize the levelized cost of the product (freshwater) regarding technical and environmental constraints. For this aim, the mathematical modeling of both systems based on the mass,

energy, and exergy conservation equations, and the economic modeling of processes is done according to the total annual cost (TAC).

Furthermore, a comprehensive analysis of the effect of the key parameters on the technical and economic performance of these two processes is carried out. One of these parameters in the MED-TVC unit is the last effect and heating steam temperature, motive steam pressure and temperature difference. In the RO process, the parameters studied include the number of membranes, the number of pressure vessels, the pressure of the feeding water, the salinity of rejected seawater, and the feed-water temperature.

2. System description

2.1. MED-TVC system

MED thermal vapor compression process compared with the widely used thermal methods such as multi-stage flash holds some advantages [29]:

- lower primary energy consumption
- lower heat transfer area
- lower capital cost
- longer life
- less corrosion
- lower scaling rate
- less pre-filtering need

According to the results obtained in Al-Sahali and Ettouney [6], the comparison of different forward, backward, and parallel-cross configurations shows the parallel-cross arrangement's superiority. Because it performs better in terms of energy consumption and gain output ratio (GOR); thus, this arrangement has also been used in this paper. Fig. 1 displays a simplified schematic of a MED-TVC unit with n effects.

This unit comprises horizontally falling evaporators, a condenser, flashing boxes, pumps, a heater, and a steam jet ejector that operates as a thermal compressor. The extracted motive steam with the mass flow rate of D_s in almost high pressure (P) is directed towards the steam jet ejector. Part of the formed steam in the final effect (D),

is drawn and compressed together with D_s by the steam jet ejector. The leaving steam from the ejector with a mass flow rate of $D_s + D_r$ is fed to the first effect. The steam at the first effect delivers its latent heat and condenses. The latent heat is used to increase the falling water temperature of the first effect from T_f to T_1 (boiling point of the first effect) and evaporates section of the feeding water (D_1). The unevaporated portion of seawater (B_1) is also collected as brine or wastewater at the bottom of the chamber and goes to the second effect. A portion of the condensate D_s goes back to its boiler or heat source, and the other part moves to the first flashing box in which some part of the vapor flashes off because of the drop in the pressure. The vapor produced in effect 1 goes to the evaporator tube bundle of effect 2 and then transfers its heat of condensation to the falling film and condenses into freshwater. As a result, part of the sprayed water turns into steam, and this steam goes to the next effect, and this process repeats until the last effect. For optimal saline water energy use, the output brine from the first effect enters the second effect to increase the feedwater temperature from T_{f_2} to T_{f_1} . The steam formed in the last effect, along with the vapor generated in the last effect, is divided into two streams. The ejector draws the first flow (D), and the second stream D_c in the condenser will lose its latent heat and condenses. In the condenser, the temperature of the seawater increases from T_{cw} to T_f . Part of the seawater with a mass flow rate of M_f is used as feed-water, and remaining with a flow rate of M_{cw} is used as the cooling water. The cooling water's main function is to eliminate the excess heat given to the system in the first effect. The motive steam that has lost its latent heat in the first effect and turned into saturated water is sent to the steam boiler to re-heat and is employed with higher pressure and temperature as the steam jet ejector's primary flow, completing the MED-TVC thermodynamic process.

2.2. RO system

The accelerated development of the RO process in recent years is due to its ability to produce freshwater at a lower cost. One of the attractive features of RO is the simplicity and modularity of the operation and design.

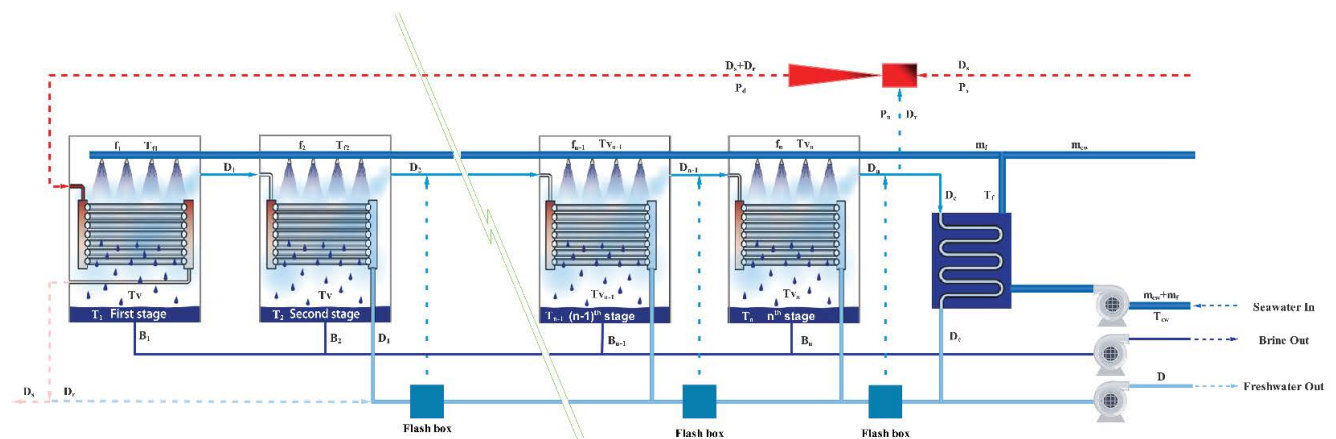


Fig. 1. A detailed illustrative of MED-TVC unit.

In this plant, the RO membrane modules are highly compacted, scaled up, and installation and replacement are relatively straightforward than thermal desalination plants. Another benefit of this process is its ability to produce freshwater with different salinity levels for a wide range of seawater and brackish water [30].

Each RO process consists of several successive stages. Usually, the number of these stages is up to 3; depending on seawater’s salinity or brackish water, the number of stages varies. The wastewater from each stage is fed to the next stage, and then the desalination operation is performed on it. Each stage in the process consists of several pressure vessels that are parallel to each other. The feeding water is divided equally between the pressure vessels at each stage. A maximum of eight membranes is placed in each vessel in series. The extracted freshwater from all membrane modules is gathered, and the wastewater from the first membranes is fed as the supply water to the second membrane, and this process proceeds to the final membrane modulus, and eventually, the wastewater from the last module is returned. The wastewater from all pressure vessels is removed from the first stage as wastewater, but again as the feed water is fed to the next stage, and at that stage, the desalination process is performed on it. Since wastewater from the RO system contains a high-value of potential energy, an energy recovery system is often used at the wastewater outlet to increase the efficiency and economic performance of the process. Fig. 2 illustrates a schematic of an RO unit.

3. Mathematical modeling

3.1. Thermodynamic modeling

For a technical analysis of the MED-TVC and RO desalination plants, it is necessary to apply thermodynamic

modeling based on the mass and energy conservation equations.

3.1.1. MED-TVC system

For the mathematical modeling of the MED-TVC process, the following assumptions are made [31,32]:

- All the processes are considered steady state.
- The thermal loss to the ambient is negligible since the condensers and evaporators are insulated.
- The temperature difference between the effects is same.
- The salinity of the finally rejected flow is considered to be 70,000 ppm.
- The produced freshwater is assumed to be salt-free.
- Overall feed flow rate is equally divided between all effects ($f_1 = f_2 = \dots = f_N = F/N$).

As mentioned earlier in the assumption, the temperature difference between the effects is constant; hence, for the n number of effects, the temperature difference is calculated as follows [33]:

$$T_{i-1} - T_i = \Delta T = \frac{T_1 - T_n}{n - 1} \tag{1}$$

$$T_1 = T_d - \Delta T \tag{2}$$

Herein, T_d refers to the temperature of the leaving steam from the ejector or the heating steam temperature at the first effect. T_1 and T_n denotes to the temperature of the first and last effect, respectively [33].

The mass and energy conservation equations in the ejector are presented as follows [34]:

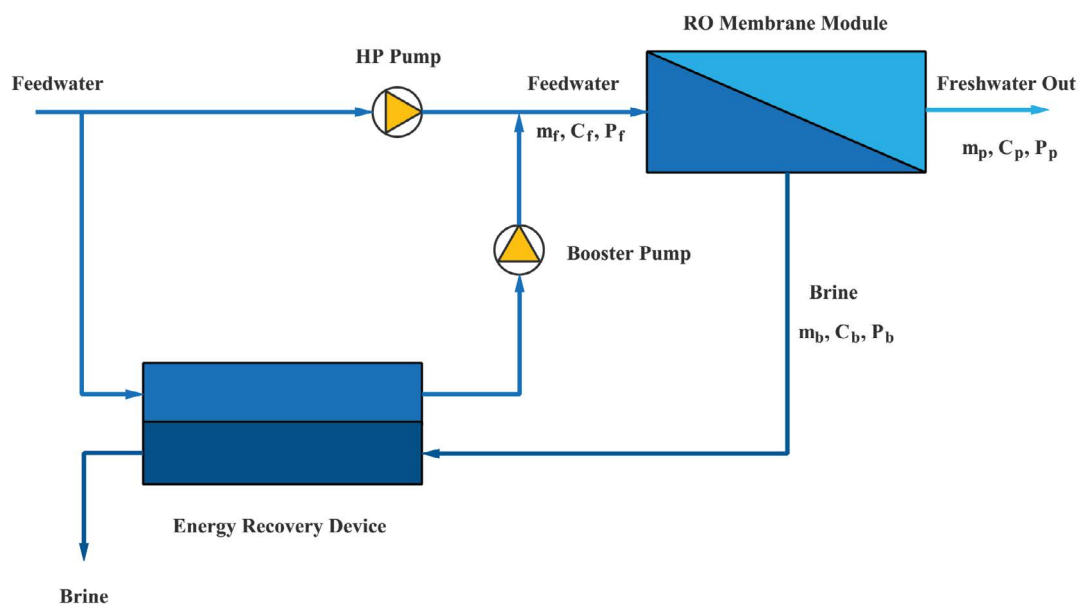


Fig. 2. Schematic of the RO system.

$$D_0 = D_r + D_s \quad (3)$$

$$\omega = \frac{D_r}{D_s} \quad (4)$$

$$h_d = \frac{h_s + \omega h_{sn}}{1 + \omega} \quad (5)$$

Therein, D_s is the motive steam mass flow rate which is sent to the ejector as the primary flow from boiler and D_r stands for the mass flow rate of entrainment steam from the last effect. The temperature and pressure of the entrainment flow increase in the mixing section of the ejector. Also, ω is the mass entrainment ratio of the ejector, which is obtained within the following semi-empirical relation [34]:

$$\omega = \frac{D_s}{D_r} = \frac{0.296 P_d^{1.19}}{P_n^{1.04}} \times \text{ER}^{0.015} \left(\frac{\text{PCF}}{\text{TCF}} \right); \quad \frac{D_s}{D_r} \leq 4 \quad (6)$$

where P_d and P_n are the pressures of the compressed vapor and entrained vapor, respectively, PCF is the motive steam pressure correction factor, and TCF is the entrained vapor temperature correction factor [34].

$$\text{PCF} = 3 \times 10^{-7} P_s^2 - 0.0009 P_s + 1.6101; \quad 100 \text{ kPa} \leq P_s \leq 3,500 \text{ kPa} \quad (7)$$

$$\text{TCF} = 2 \times 10^{-8} T_{vn}^2 - 0.0006 T_{vn} + 1.0047; \quad 10 \leq T_{vn} \leq 500^\circ \text{C} \quad (8)$$

$$\text{CR} = \frac{P_d}{P_n}; \quad \text{CR} \geq 1.81 \quad (9)$$

$$\text{ER} = \frac{P_s}{P_n} \quad (10)$$

where P_s is the pressure of the motive steam in kPa and T_{vn} is in $^\circ\text{C}$. CR and ER are the compression ratio and expansion ratio. The previous equations are valid only for ejectors operating with steam as the motive fluid and the entrained gas is water vapor.

The feed seawater flow rate is divided equally to all effects at a rate equal to F_i into effects.

$$F_i = \frac{F}{N} \quad (11)$$

For the effects, the rejected mass flow rate can be defined based on the mass balance law as follows [32]:

$$B_1 = F_1 - D_1 \quad (12)$$

$$D_1 = \frac{[D_0(h_d - d_{fd}) - F_1 C_p (T_1 - T_F)]}{\lambda_1} \quad (13)$$

where B_1 is the rejected mass flow rate of the first effect, D_1 is the mass flow rate of formed steam at the first effect, and λ represents the specific latent heat for evaporation.

The salt's mass balance for the first effect is presented as follows [32]:

$$X_{b_1} = \frac{F_1}{F_1 - D_1} X_F \quad (14)$$

Herein, X_F and X_{b_i} indicate the salinity of the supply saline water and the salinity of the rejected brine, respectively. With increasing the salinity of the water, the boiling point temperature increases; thus, the temperature of the generated vapor in each effect is lower than the boiling point of that effect. Therefore, the vapor temperature of the i th effect is given by [32]:

$$T_{v_i} = T_i - \text{BPE}_i \quad (15)$$

Herein, BPE stands for boiling point elevation, and T_v is the vapor temperature.

From the second effect, the steam is formed by the aim of two mechanisms, one is the evaporation, and the other is flashing. Part of the rejected brine of the previous effect evaporates due to the pressure decrement in flash boxes [33].

$$D'_i = \frac{D_{i-1} C_p (T_{v_{i-1}} - T_i)}{\lambda_i}; \quad i = 2, 3, \dots, n \quad (16)$$

The conservation of mass and energy for the i th effect is written as follows [32]:

$$D_i = \frac{(D_{i-1} + D'_{i-1}) \lambda_{i-1} - F_i C_p (T_i - T_F) + B_{i-1} C_p (T_{i-1} - T_i)}{\lambda_i} \quad (17)$$

$$B_i = B_{i-1} + F_i - D_i = (B_{i-2} + F_{i-1} - D_{i-1}) + F_i - D_i = \sum_{k=1}^i F_k - D_k \quad (18)$$

In the above equation, D_i is the amount of vapor formed in effect i , D' is the amount of vapor formed by flashing in the flashing boxes, λ is the latent heat, C_p is the specific heat at constant pressure, T_i is the brine boiling temperature, and T_f is the feed seawater temperature [32].

$$X_{b_i} = \frac{X_F F_i + X_{b_{i-1}} B_{i-1}}{B_i} \quad (19)$$

where B and F are the flow rates of brine and feed water, X is the salinity, and the subscripts F and i designate the feed and the effect number. The flow rate of cooling water is calculated through the following relation [32]:

$$D_c = D_n + D'_n - D_r \quad (20)$$

$$(M_{cw} + M_f) C_p (T_F - T_{cw}) = D_c \lambda_n \quad (21)$$

For evaluation of heat transfer area, the below equations are applied [32].

$$A_1 = \frac{D_0(h_d - h_{fd})}{U_1(T_d - T_1)} \quad (22)$$

$$A_i = \frac{(D_{i-1} + D'_{i-1})\lambda_{i-1}}{U_i(\Delta T)} \quad (23)$$

The total heat transfer coefficient for the evaporator is obtained using the following semi-empirical relation. In this relation, the temperature is based on °C [32].

$$U_i = \frac{1939.4 + 1.40562T_i - 0.0205725T_i^2 + 0.0023186T_i^3}{1,000} \left[\frac{\text{kW}}{\text{m}^2\text{°C}} \right] \quad (24)$$

$$A_e = A_1 + A_2 + A_3 + \dots + A_n = \sum_{i=1}^n A_i \quad (25)$$

The heat transfer area for the condenser is obtained by using the following equation [32]:

$$A_c = \frac{D_c \lambda_n}{U_c (\text{LMTD})_c} \quad (26)$$

where A_c , U_c , and $(\text{LMTD})_c$ are the heat transfer area, overall heat transfer coefficient, and logarithmic mean temperature difference. Also, the total heat transfer coefficient for the condenser is calculated based on the following relation [32]:

$$U_c = 1.7194 + 3.2063 \times 10^{-3} T_{v_n} + 1.5971 \times 10^{-5} T_{v_n}^2 - 1.9918 \times 10^{-7} T_{v_n}^3 \quad (27)$$

The total generated distilled water for the MED-TVC unit [32]:

$$D_{\text{tot}} = \sum_{i=1}^n D_i \quad (28)$$

The total value of the fuel consumption rate can be described as follows [32]:

$$\eta_{\text{boiler}} \times \dot{m}_{\text{fuel}} \times \text{LHV} = D_s \times (h_s - h_{fd}) \quad (29)$$

An important parameter of the thermal desalination units is the GOR, which is the ratio of the generated distilled water mass to the motive steam flow rate:

$$\text{GOR} = \frac{D_{\text{tot}}}{D_s} \quad (30)$$

On the other hand, the specific heat consumption (Q_d) rate and the specific heat transfer area (A_d) are obtained according to the following relations [32]:

$$Q_d = \frac{D_s \lambda_s}{D_{\text{tot}}} \quad (31)$$

$$A_d = \frac{A_e + A_c}{D} \quad (32)$$

The mathematical modeling of the MED-TVC unit from Eqs. (1)–(32) was carried out applying EES (Engineering Equation Solver) software. The solution algorithm of the thermal vapor compression system is presented in Fig. 3a.

3.1.2. RO system

There have been developed numerous models for performance analysis of the RO systems. To design and optimize the RO system, it is essential to apply the most proper models that can desirably forecast the membrane performance. The solution-diffusion model is one of the mostly used methods for the RO system analysis. This model is constructed according to two main parameters including the permeability of the water (A) and the second parameter is the solute transport (B). The membrane manufacturing company assigns these two parameters values [30].

For modeling the RO system, the following assumptions are made.

- The process is considered to be isothermal.
- The process acts in a steady-state condition
- There are no chemical reactions within the RO unit.

In the RO desalination process, an increase in saline water temperature results in an increment in the water permeability through the membrane; hence, the pump's power decreases. The effect of temperature on the membrane permeability applies using temperature correction factor (TCF), and the fouling factor (FF) is employed to apply the fouling impact on the water permeability (A).

$$A = A_{\text{ref}} \times \text{FF} \times \text{TFC} \quad (33)$$

where, A_{ref} is the pure water permeability at $T = 25^\circ\text{C}$. The fouling factor (FF) value varies between 1 for new membranes and 0.8 for 4 y old membranes [35]. The TCF is obtained using the following equation [35]:

$$\text{TCF} = e^{\frac{e}{8.314} \left(\frac{1}{298} - \frac{1}{T+273} \right)} \quad (34)$$

In the above-mentioned relation, T is based on the °C, and the value for the membrane activation energy (e) is estimated to be 22,000 for $T > 25^\circ\text{C}$, and 25,000 for $T \leq 25^\circ\text{C}$ [36].

The permeate mass flow rate is equal to [35]:

$$\dot{m}_p = (J_w + J_s) S_m \quad (35)$$

Herein, J_w is the permeate mass flux, J_s denotes for the salt mass flux through the membrane, and S_m is the membrane active area.

Water and salt's mass balance across the membrane is presented as follows [35]:

$$\dot{m}_f = \dot{m}_p + \dot{m}_b \quad (36)$$

$$c_f \dot{m}_f = c_p \dot{m}_p + c_b \dot{m}_b \quad (37)$$

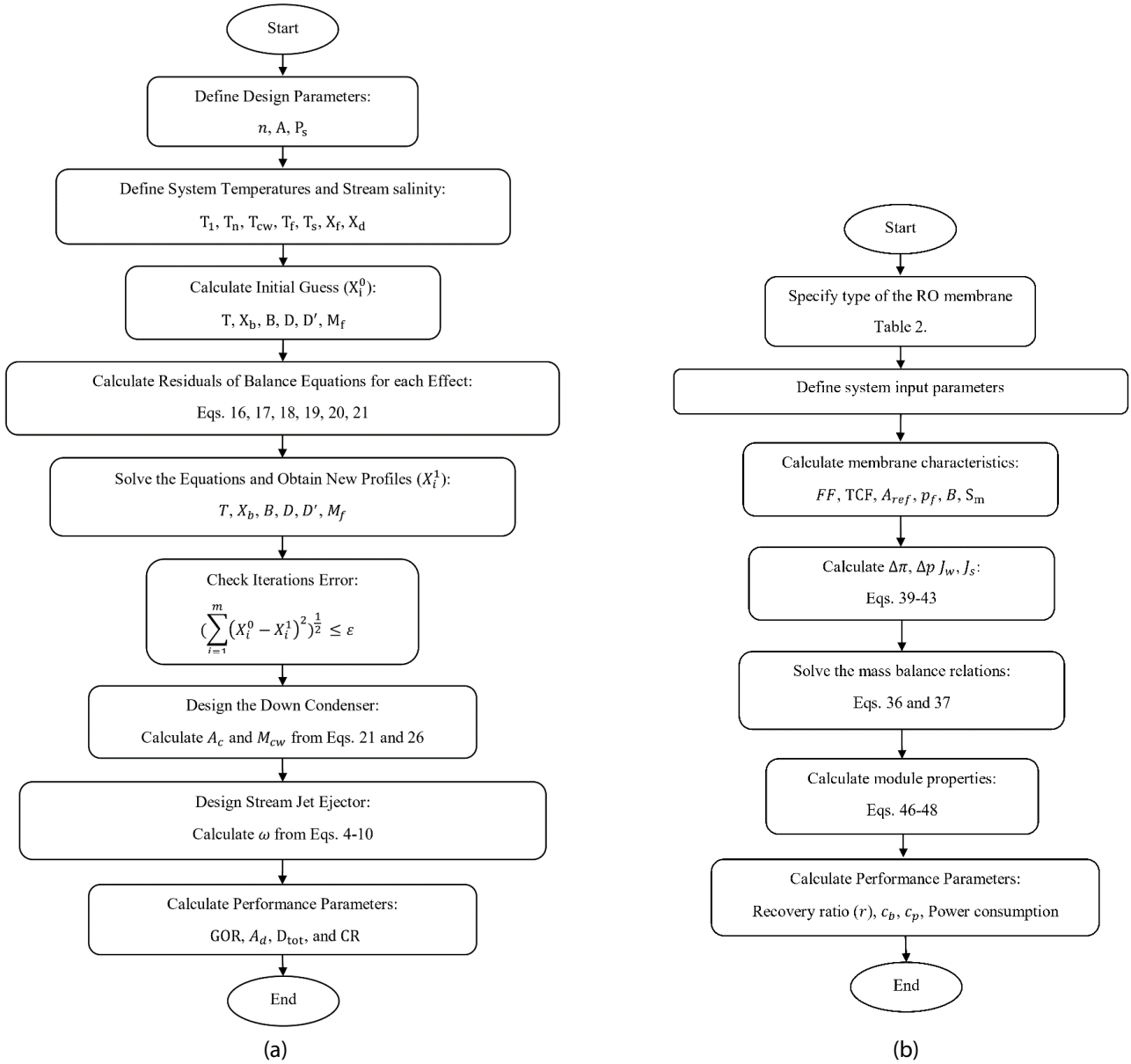


Fig. 3. Solution procedure of the (a) thermal vapor compression system and (b) reverse osmosis system.

where, c_s , c_b , and c_p are the salinity of the seawater, brine, and distilled water, respectively. The water recovery rate is described as follows [35]:

$$r = \frac{\dot{m}_p}{\dot{m}_f} \quad (38)$$

Permeate mass flux through the membrane is obtained using Fick's law [35]:

$$J_w = A(\Delta p - \Delta\pi) \times 10^3 \quad (39)$$

Therein, A denotes for the membrane water permeability, Δp is the transmembrane pressure, and $\Delta\pi$ is the osmotic

pressure across the membrane. Salt mass flux across the membrane is equal to [35]:

$$J_s = \frac{B(c_w - c_p)}{10^6} \quad (40)$$

where B is the salt permeability of the membrane, c_w is salinity in the membrane wall. The following relationships are used to obtain the transmembrane pressure, the pressure drop across the membrane, and osmotic pressure across the membrane [35].

$$\Delta p = p_f - p_p - \frac{\Delta p_f}{2} \quad (41)$$

$$\Delta p_f = 9.5 \times 10^5 \left(\frac{\dot{m}_f + \dot{m}_b}{2\rho} \right)^{1.7} \quad (42)$$

$$\Delta\pi = 2 \times \frac{8.314}{0.0585} \times (T + 273.15) \times \frac{\rho(c_w - c_p)}{10^9} \quad (43)$$

where ΔP is the transmembrane pressure, p_f is the applied feed pressure, p_p is the resulting permeate pressure, Δp_f is the pressure drop along the membrane channel. \dot{m}_f is the membrane feed flow rate, \dot{m}_b is the membrane concentrate flow rate.

Also,

$$J_s = \frac{J_w c_p}{10^6} \quad (44)$$

The concentration polarization must be regarded in the modeling process since this phenomenon results in a decrement in the water production rate. By applying the concentration polarization effects, the following equation can be used to obtain the wall salinity [35]:

$$c_w - c_p = \left(\frac{c_f + c_b}{2} - c_p \right) e^{k \cdot r} \quad (45)$$

Herein, r is the recovery rate, k is the mass transfer coefficient, which considered 0.7 for spiral membrane in this study [35]. Since in each pressure vessel, the membrane modules are arranged in series, the following equations are used for 2nd to i th module [36].

$$\dot{m}_f(i) = \dot{m}_b(i-1); \quad i = 2, \dots, m \quad (46)$$

$$c_f(i) = c_b(i-1); \quad i = 2, \dots, m \quad (47)$$

$$p_f(i) = p_f(i-1) - \frac{\Delta p_f(i-1)}{2}; \quad i = 2, \dots, m \quad (48)$$

The solution algorithm of the RO system is presented in Fig. 3b.

3.2. Techno-economic modeling

For the economic analysis of the proposed desalination systems, it is essential to evaluate the TAC. The TAC for RO and MED-TVC systems including annual capital cost (ACC), annual operating cost (AOC), and annual maintenance cost (AMC) [37].

$$\text{TAC} = \dot{C}_{\text{ACC}} + \dot{C}_{\text{AOC}} + \dot{C}_{\text{AMC}} \quad (49)$$

The ACC is a function of the equipment purchase cost and the economic parameters of the country such as inflation rate [37].

$$\dot{C}_{\text{ACC}} = C_{\text{Equipment}} \times \text{CRF} \quad (50)$$

where CRF denotes for the capital recovery factor, which is defined as follows [37]:

$$\text{CRF} = \frac{i(i+1)^y}{(i+1)^y - 1} \quad (51)$$

$$i = \frac{j-f}{1+f} \quad (52)$$

Herein, i is the real interest rate, j represents the nominal interest rate, and f is the annual inflation rate. The equipment cost in the MED-TVC is comprising the purchase cost of evaporators, ejectors, condensers, boilers, and pumps [37].

$$C_{\text{Equipments}} = Z_{\text{Evaporators}} + Z_{\text{Ejector}} + Z_{\text{Cond}} + Z_{\text{Pumps}} + Z_{\text{Boiler}} \quad (53)$$

In the RO, the equipment's cost, including pumps, energy recovery system, and permeators (membrane and pressure vessels).

$$C_{\text{Equipment}} = Z_{\text{Permeator}} + Z_{\text{Pumps}} + Z_{\text{ers}} \quad (54)$$

The operation cost of the plant includes annual cost of fuel consumption, electricity utilization, insurance, chemical processing of the water, and replacement cost of the equipment.

The replacement cost for the MED-TVC unit is considered zero while for the RO system, this value for every 5 y is calculated through the following equation [37]:

$$\dot{C}_{\text{Rep}} = m \times c_{\text{mem}} \times \text{num}_{\text{pv}} \times \frac{j \times (1+i)^{y_{\text{rep}}}}{(1+i)^{y_{\text{rep}}} - 1} \quad (55)$$

The most critical parameters for the economic analysis are presented in Table 1.

The cost for the chemical processing of the produced water in the RO system is evaluated through [37]:

$$\dot{C}_{\text{che}} = \dot{m}_{\text{feed}} \times 3.6 \times 24 \times 365 \times 0.9 \times 0.018 \quad (56)$$

And for the MED-TVC unit [37]:

$$\dot{C}_{\text{che}} = 0.0315388 \times D_{\text{tot}} \times 3.6 \times (0.9 \times 365 \times 24) \quad (57)$$

The levelized cost of the product for the water is described as follows [37]:

$$\text{LCOP}_{\text{water}} = \frac{\text{TAC}}{\text{annual fresh water production}} \quad (58)$$

Since, the levelized cost of the product is not a proper criterion for comparison between the market price and water price because the LCOP value is according to all costs in the life of the project, hence; describing an appropriate parameter for comparing with the market price is necessary. For this aim, prime cost is introduced. For evaluation of the prime cost, first of all, operating flow costs (OFC) is calculated as follows [37]:

Table 1
Required parameters for the parametric and economic study

Parameter	Value	Unit
Feedwater salinity	42,000	ppm
Seawater temperature	30	°C
Seawater density	1,020	kg/m ³
LHV	50,047	kJ/kg
Electricity price	0.0154	USD/kWh
Fuel price	0.02898	USD/m ³
Water price	1.5	USD/m ³
Maintenance and repair cost	5% of the total capital cost	–
Installation cost	10% of components cost	–
Insurance cost	2% of capital cost	–
Plant lifetime	20	years
Accessibility coefficient	0.9	–

$$\text{OFC} = \dot{C}_{\text{op}} + C_{\text{maintenance}} \quad (59)$$

The prime cost value is the ratio of the OFC to the yearly product volume (VOP) and is defined as follows [37]:

$$\text{PC} = \frac{\text{OFC}}{\text{VOP}} \quad (60)$$

Besides, the capital cost is the summation of the installation cost and the purchase cost of components.

Summation of product cost (SOPC) is defined as the annual income through water selling. The net annual benefit is defined as follows [37]:

$$\text{NAB} = \text{SOPC}_{\text{water}} - \text{OFC} - \text{TAX} \quad (61)$$

And,

$$\text{POR} = \frac{\text{CC}}{\text{NAB}} \quad (62)$$

3.3. Input parameters

For a parametric and economic analysis of the desalination plants, some known parameters are given in Table 1.

4. Optimization methodology

For the optimization process, the PSO is selected. The proposed PSO algorithm is a meta-heuristic algorithm, which is a nature-inspired algorithm established based on the swarm behavior of bird and fish flock movement. Due to its many advantages including its simplicity and easy implementation, the algorithm can be used widely in the fields such as function optimization, model classification, machine study, neural network training, signal procession, vague system control, automatic adaptation control, etc. The PSO algorithm searches the solution space by adapting the particles' trajectories [38].

The main advantages of the particle swarm optimization algorithm are [39] as follows:

- PSO is an intelligent-based algorithm. It can be employed in both scientific research and engineering use.
- PSO has no overlapping and mutation calculation. The speed of the particle can carry out the search. During the development of several generations, only the most optimist particle can transmit information onto the other particles, and the speed of the research is breakneck.
- The calculation in PSO is straightforward. Compared with the other developing calculations, it occupies a more significant optimization ability, and it can be completed efficiently.
- PSO adopts the real number code, and it is decided directly by the solution. The number of the dimension is equal to the constant of the solution.

On the other hand, some disadvantages of the PSO algorithm can be stated as follows [39]:

- The method easily suffers from partial optimism, which causes the less precise regulation of its speed and direction.
- The method cannot work out the problems of scattering and optimization.
- The method cannot work out the non-coordinated system's problems, such as the solution to the energy field and the particles' moving rules in the energy field.

The optimization process through the PSO algorithm is shown in Fig. 4.

The objective function is assigned levelized cost of the product, which should be minimized in the optimization process for the production of 3,000 m³/d potable water for both MED-TVC and RO systems. Some of the constraints for the optimization is given as follows, which should be satisfied in the optimization process.

- The maximum allowed salt concentration in the distilled water is considered 350 ppm.
- The maximum allowed rejected saline water for both RO and MED-TVC units is regarded 70,000 ppm.
- The minimum GOR value for MED-TVC system is 8.

- The maximum input water pressure for the RO system depends on the membrane's allowable pressure.

Besides, for evaluation of the RO system, the characteristics of three well-known membranes, namely: SW30XLE-40, SW30HR-380, SW30HR-320 is used and presented in Table 2 [30].

The effective parameters for minimization of the LCOP in the RO system comprising feed water pressure, type of employed membrane, number of pressure vessels, and number of membranes. Also, for MED-TVC unit, last effect temperature, heating steam temperature, motive steam pressure, feed water temperature, and the number of effects are regarded as the decision variables.

5. Results and discussion

In this part of the paper, the results of the simulation for the proposed systems are presented. First, to guarantee the results are obtained, it is necessary to evaluate the validity of the models with the previous works.

5.1. Validation

In order to prove the validity of the obtained results achieved from the mathematical evaluation of the proposed desalination systems, the EES software is employed to expand a proper Cde. The validation of the obtained results is carried out with two previously published articles for the MED-TVC and RO units. The validation of the models followed the following procedures:

To validate the MED-TVC, Table 3 is provided. The table listed some of the main parameters of each effect for the present study and the work of Bin Amer [32]. The input parameters for the comparison are set similar to the reference data. As Table 3 presents, the results are in good agreement with the outcomes of Bin Amer [32].

The obtained parameters of each membrane of the RO are validated with the results of Vince et al. [35]. The results for authentication of the RO are presented in Table 4, which shows high accordance with the data of Vince et al. [35].

5.2. Parametric study

Parametric studies provide some advantages such as a specification of parameters for assessment, parameter range determination, the definition of the design limitations, and investigation of the effects of various parameters change on the specific problem.

5.2.1. Multi-effect desalination thermal vapor compression

5.2.1.1. Effect of the number of effects on technical criteria of MED-TVC

Fig. 5a illustrates the number of effects impact on the technical performance criteria of the MED-TVC unit. As shown in this figure, increasing the number of effects results in a considerable increment in the GOR value due to an increase in distilled water production. Also, by

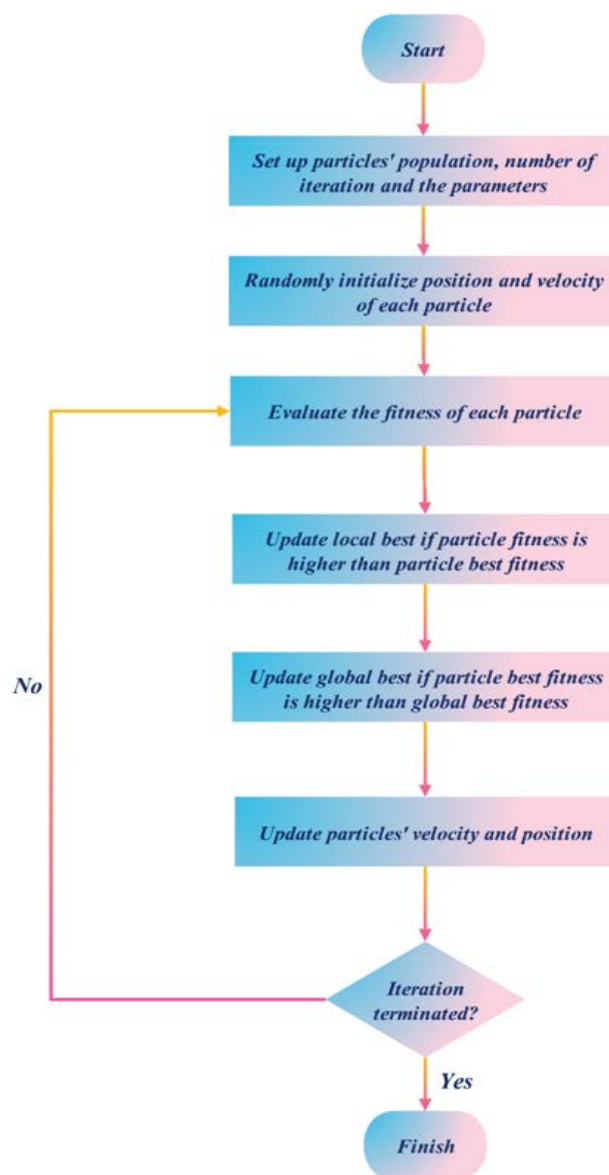


Fig. 4. Flowchart of the optimization process through the PSO algorithm.

increasing the number of effects, the heat transfer area increases; hence, the specific heat transfer area rises, which means that the rate of increment of heat transfer area is higher than the water production rate. Besides, the specific heat decreases since the input heat value remains constant while the water production rate increases.

5.2.1.2. Influence of effect number on the period of return (POR) and levelized cost of the product

The effect's number impact on the economic parameters is manifested in Fig. 5b. According to Fig. 5b illustrations, an increase in the number of effects has a negative influence on the economic metrics since an increase in n leads to increasing the payback period and LCOP of water. It is due to the fact that increasing number of effects

Table 2
Specifications of RO membranes used in modeling

Parameter	Unit	Membrane type		
		SW30XLE-400	SW30HR-380	SW30HR-320
Active area (s_m)	m ²	37.2	35.3	29.7
Maximum operating pressure (p_f)	bar	83	83	83
Water permeability constant (A)	kg/m ² s Pa	3.5×10^{-9}	2.7×10^{-9}	3.1×10^{-9}
Salt permeability constant (B)	kg/m ² s	3.2×10^{-5}	2.3×10^{-5}	2.2×10^{-5}
Membrane cost	\$	1,200	1,000	1,400

Table 3
Verification of modeling based on the results of Reference [32]

n	Parameters											
	Temperature (°C)		CR		ER		D_s/D_r		GOR		At_d (m ² /kg/s)	
	Ref. [32]	Present work	Ref. [32]	Present work	Ref. [32]	Present work	Ref. [32]	Present work	Ref. [32]	Present work	Ref. [32]	Present work
4	46.7	46.41	1.81	1.81	248	239	0.731	0.732	8.52	8.52	485.1	484.5
5	46.1	45.9	1.81	1.81	256	246	0.731	0.731	10.16	10.44	712.4	710.15
6	44.3	42.71	1.98	1.97	281	270	0.8	0.800	11.49	11.82	596.6	597.2
7	42.8	40.5	2.20	2.20	304	292	0.897	0.897	12.66	12.85	559.1	560.23
8	42.8	40.4	2.46	2.45	304	292	1.025	1.025	13.68	13.79	505.5	504.12

Table 4
Comparison and validation of the developed model with [35]

Membrane No.	Parameters							
	J_w (kg/m ² s)		\dot{m}_f (m ³ /h)		x_f (g/L)		Δp (bar)	
	Ref. [35]	Present work	Ref. [35]	Present work	Ref. [35]	Present work	Ref. [35]	Present work
1	27.9	27.9	9.3	9.3	3	3	11.4	11.4
2	26.1	26.1	8.2	8.2	3.4	3.4	11.2	11.3
3	24.1	24.1	7.1	7.1	3.9	3.9	11	11.2
4	21.6	21.7	6.1	6.2	4.6	4.5	10.8	11.1
5	18.8	18.8	5.3	5.3	5.4	5.3	10.7	10.9
6	15.7	15.7	4.5	4.5	6.3	6.1	10.5	10.8
7	12.3	12.3	3.9	3.9	7.4	7.1	10.3	10.5

results in higher heat transfer area, and because the cost functions of MED-TVC unit are based on the heat transfer area, thus, it can be concluded that one of the determinative parameter in the MED-TVC unit from the economic aspects is the specific heat transfer area. With increment of number of effects, the heat transfer area and cost of MED-TVC unit increases. As a result, the POR and LCOP increases.

5.2.1.3. Effect of temperature difference of effects on the technical parameters in MED-TVC system

Fig. 6 is plotted to clarify the change of the technical parameters of the MED-TVC system with variation in the temperature difference of effects. With increasing

the temperature difference, the water production rate decreases. The reason behind this fact is that as the temperature increases, the heat transfer area decreases and then the water production rate in each effect decreases, and since the mass flow rate of motive steam is constant, the GOR value diminishes. Because the supply heat quantity is fixed and the water production rate is reduced, the specific heat is increased. The rise in temperature difference caused a drop in the heat transfer area and ultimately in the specific heat transfer area. The increment of temperature difference has a negative effect on plant performance since the water production rate decreases in each effect. On the other hand, from the economic viewpoint, it can be stated that the increment of temperature difference leads

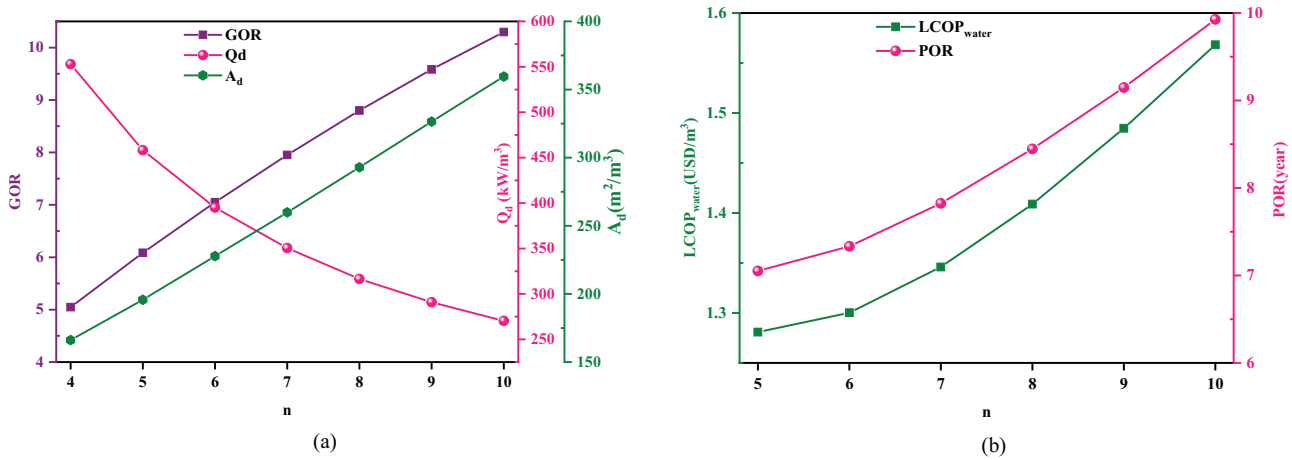


Fig. 5. Effect of the number of effects on (a) technical criteria of MED-TVC and (b) period of return and production cost.

to a lower specific heat transfer area. Due to the effect of the heat transfer area on the cost functions, the purchase cost decreases; hence, the effect of temperature difference increase on the economic parameters is positive.

5.2.1.4. Effect of ejector compression ratio on technical parameters

Fig. 7 represents the effect of ejector’s compression ratio on the technical metrics of the MED-TVC system. An augmentation in compression ratio results in a reduction in GOR. The effect of compression ratio is similar to the influence of the temperature of the motive steam temperature since the rise in the compression ratio, ejector’s exhaust pressure, and temperature increases. Therefore, it can result that increasing the compression ratio or temperature of ejector harms the system performance. The logic behind this point is that the rise in the compression ratio leads to an increase in temperature differences of the effects, which result in GOR reduction as discussed before.

5.2.1.5. Effect of the last effect temperature on the economic metrics

Fig. 8 is plotted to depict the impact of the last effect temperature on the levelized cost of product and the TAC of the MED-TVC unit. Rising the temperature of the last effect causes an increase in TAC, which results from the rise of the heat transfer area in the evaporators. Besides, enhancing the last effect temperature decreases the temperature difference in the effect and then the GOR value and the specific heat transfer area increase so that the TAC and LCOP values go up.

5.2.1.6. Effect of motive steam pressure on the operation of the system

Fig. 9a illustrates the effect of motive steam pressure as the primary flow pressure in the ejector on the entrained ratio (ω) and total water production rate. For extracting this figure, the number of effects is set 6, the motive

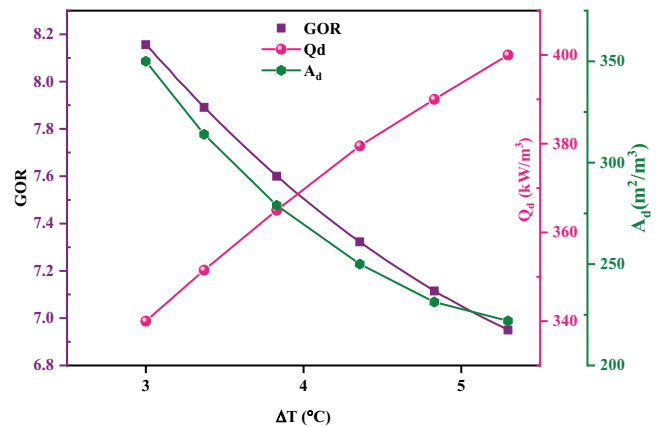


Fig. 6. Effect of temperature difference of effects on the technical parameters in MED-TVC system.

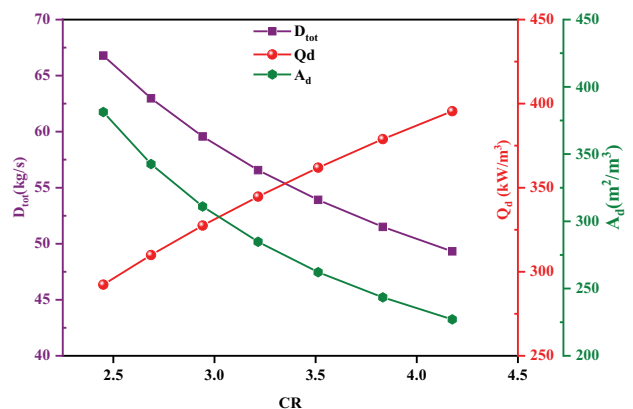


Fig. 7. Impact of ejector compression ratio on technical parameters.

steam’s mass flow rate is regarded 7 kg/s, the temperature of heating steam is considered 70°C, and the temperature of the last effect is set 40°C. With consideration of this constant value, increase in motive steam pressure,

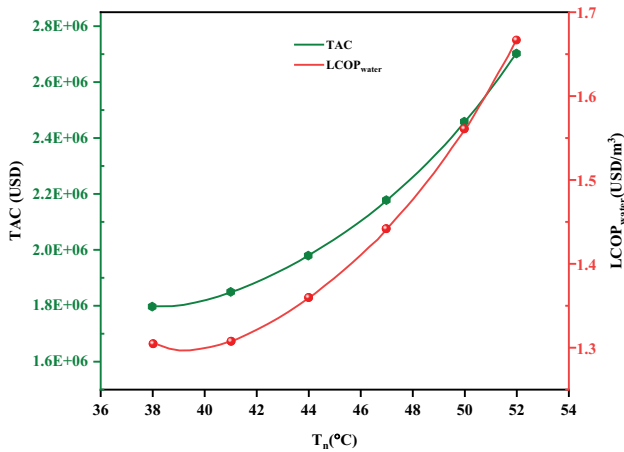


Fig. 8. Impact of the last effect temperature on the economic metrics.

the entrained ratio increases to a particular value and then drops. Besides, increasing the motive steam pressure effects similar to ω on the water production rate. The reason for these trends can be presented as; according to mentioned relations for ejector modeling, the entrainment ratio (ω) is a function of different parameters, one of them is p_s . p_s appears in two different parameters, including ER and PCF. According to Eq. (7), PCF is a function of p_s , and also, ER defined as $ER = p_s/p_n$. Hence, interaction of these two parameters effects the entrainment ratio. Therefore, increasing motive steam pressure, first increases the entrainment ratio and then decreases.

Moreover, the impact of motive steam pressure on the capital cost (CC) and the POR is displayed in Fig. 9b. As can be seen, at the point of operation, the highest value of capital cost is obtained. The reason behind this fact is that the increase in motive steam pressure, boiler price for generation of a fixed quantity of saturated vapor rises, on the other hand; total area has an increasing and then decreasing trend, and since the effect of area

on the capital cost is considerable, so the capital cost has an increasing and then decreasing trend. Furthermore, the POR for the MED-TVC unit enhances as the motive steam pressure rises.

5.2.2. Reverse osmosis

5.2.2.1. Effect of membrane's number on brine and permeate salinity and economic parameters

Fig. 10a illustrates the change in the brine and permeate salinity with respect to increment in the number of membranes in the RO system. With consideration of fixed value for other parameters such as the number of pressure vessels, feed water pressure, and feed water mass flow rate, any increase in the number of membranes leads to an increment in brine and permeate salinity.

On the other hand, the effect of the membrane's number on economic metrics is displayed in Fig. 10b. Based on this figure, as the number of membranes increases, the levelized cost of product and production cost for water decreases, and the water production rate increases. Thus, it can be inferred that the number of membranes in RO desalination system is a determinative factor for enhancing the technical and economic performance, while the only limitation in this aim is the allowable value of brine and permeate salinity.

5.2.2.2. Effect of the number of pressure vessels on the economic criteria

Besides the number of the membranes, the number of pressure vessels effect on the RO performance is crucial since the mass flow rate of the feed water divides among the pressure vessels. Therefore, the effect of the number of pressure vessels is depicted in Fig. 11. With increasing the number of pressure vessels, the product cost of the water remains constant, while the value of Net Annual Benefit is increased, and also the levelized cost decreases. So, similar to the effect of the membrane's number, the increase in

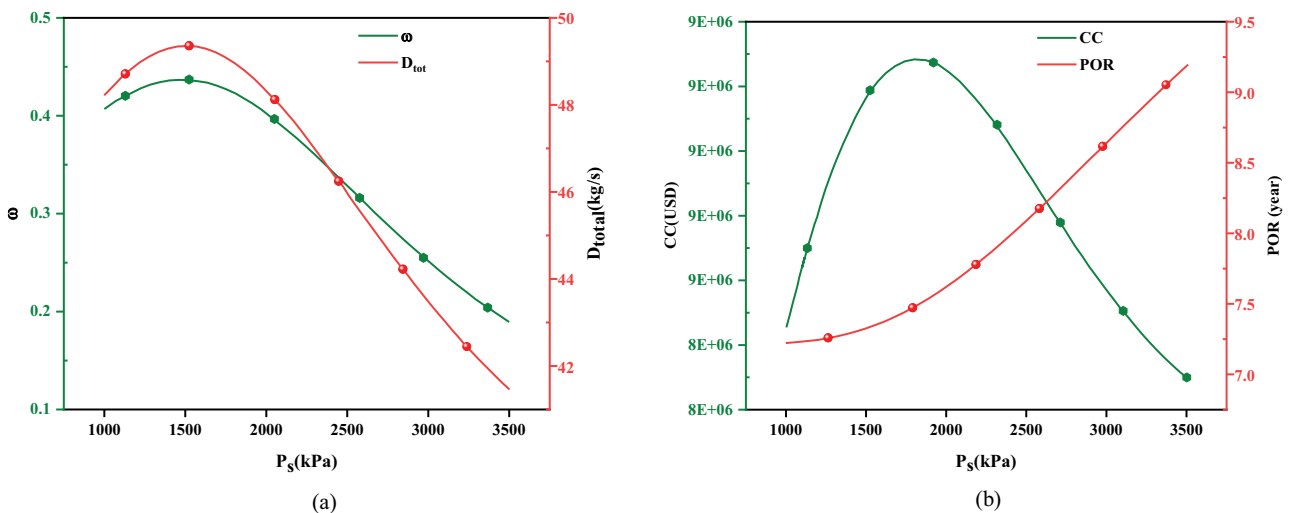


Fig. 9. Effect of motive steam pressure on (a) the operation of system and (b) the capital cost and the period of return.

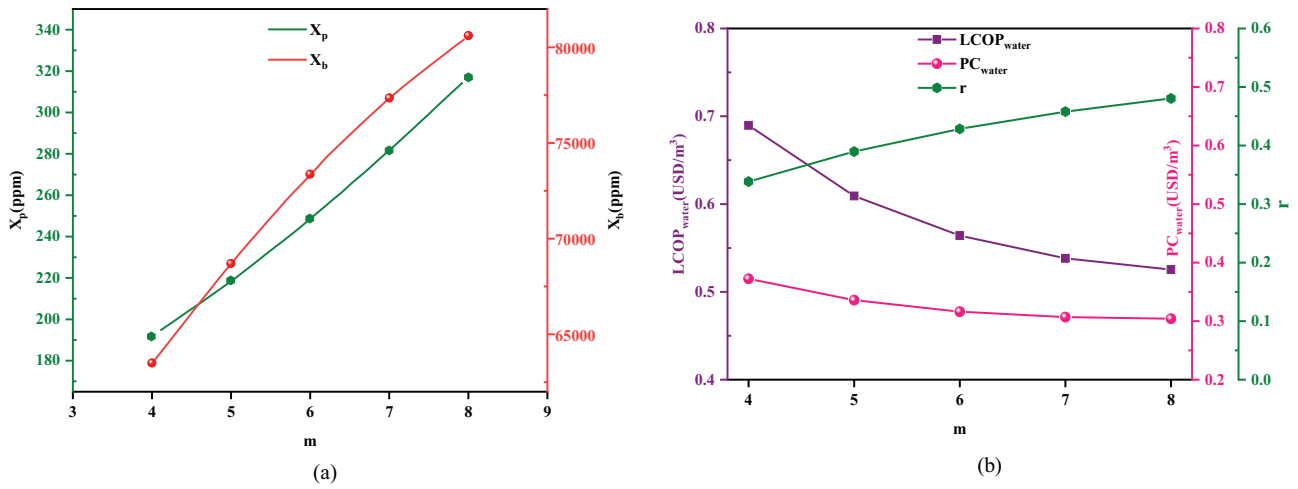


Fig. 10. Effect of membrane's number on (a) brine and permeate salinity and (b) economic metrics.

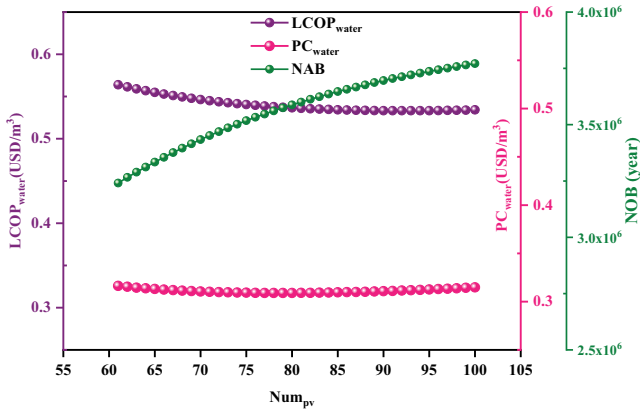


Fig. 11. Effect of the number of pressure vessels on the economic criteria.

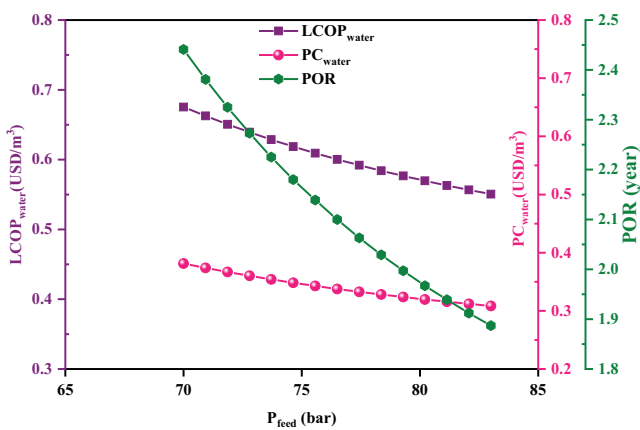


Fig. 12. Effect of feed water pressure on the economic performance of the system.

the number of pressure vessel has a positive effect on economic performance. It should be noted that the rise in the number of the pressure vessel also leads to an increment in the brine and permeate salinity. Thus, the number of

pressure vessels can be increased to an allowable limit where the brine and permeate salinity do not increase.

5.2.2.3. Effect of feed water pressure on the economic performance of the system

The effect of feed water pressure is presented in Fig. 12. Increasing the feed water pressure enhances the quantity of the produced water, while the salinity of the brine increases. According to Fig. 12, increasing the feed pressure has a perfect influence on the economic performance of the RO plant. With rising the feed pressure, the mass flow rate of produced water increases; therefore; the production cost of water for 1 m³ decreases. Also, the levelized cost and POR consequently drop.

5.3. Optimization results

The results of the optimization of both MED-TVC and RO systems are given in Tables 5 and 6. The optimization process is carried in MATLAB software using the PSO. Based on Tables 5 and 6, the most important parameter in the determination of economic performance for both plants is the price of fuel and electricity. The RO system is far better than MED-TVC system from the economic viewpoint. However, the consumption of power is higher, and the quality of the produced water is lower comparing with MED-TVC unit, but the production cost is lower and the POR is better for the RO system. Hence, it is better to combine the MED-TVC unit with other thermal systems such as Bryton cycle and solar systems to decline the costs of fuel consumption and the costs of water production.

6. Conclusion

This paper aims to evaluate and compare the technical and economic performances of MED-TVC and RO desalination systems for producing 3,000 m³ potable water per day in the same technical and techno-environmental constraints. Both systems' technical analysis is carried out based on the mass and energy and economic perspective.

Table 5
Obtained results at the optimum MED-TVC system

Parameter	Value	Unit
Number of effects (n)	8	-
Last effect temperature (T_n)	38.48	°C
Feedwater temperature (T_f)	35	°C
Heating steam temperature (T_d)	74.08	°C
Motive steam pressure (P_s)	1,239	kPa
Specific heat transfer area (A_d)	250.3	(m ² /m ³)
Specific heat transfer (Q_d)	348.2	kW/m ³
Feedwater mass flow rate (M_f)	86.81	kg/s
Entrainment ratio of ejector (ω)	0.3202	-
Gain output ratio	8	-
Compression ratio of the ejector (CR)	5.451	-
Motive steam flow rate (D_s)	4.35	kg/s
Equipment cost ($C_{\text{Equipment}}$)	6.12×10^6	USD
Levelized cost of the product (LCOP _{water})	1.339	USD/m ³
Period of return	7.763	year
Product cost (PC _{water})	0.5216	USD/m ³

Table 6
Obtained results at the optimum RO system

Parameter	Value	Unit
Membrane numbers (m)	6	-
Number of pressure vessels (Num _{pv})	21	-
Feedwater pressure (P_{feed})	77.78	bar
Type of membrane	SW30XLE-400	-
Levelized cost of the product (LCOP _{water})	0.895	USD/m ³
Period of return	3.864	Year
Product cost (PC _{water})	0.4642	USD/m ³
Feed water mass flow rate (\dot{m}_{feed})	86.52	kg/s
Rejected brine salinity (X_b)	69,985	ppm
Permeate salinity (X_p)	255.5	ppm
Recovery rate (r)	40.13	%
Equipment cost ($C_{\text{Equipment}}$)	3.23×10^6	kg/s

Optimization of both systems is performed to minimize the levelized cost of the product applying the PSO algorithm. Furthermore, a parametric study is conducted to investigate the effect of important parameters of both systems on the technical and economic performance. The results of the optimization indicate that the payback time is 3.86 and 7.76 y for RO and multi-effect thermal vapor compression units, respectively. Regarding the obtained data from the parametric analysis indicate that the RO system requires more power for potable water production and the quality of produced water is lower compared with the MED-TVC unit. Still, the RO unit is more practical from the economic viewpoints. Hence, it is better to combine the MED-TVC unit with other thermal systems such as the Bryton cycle and solar systems to reduce fuel and water

production costs. Therefore, the MED-TVC process can be driven by the waste heat of power plants and combined cycles to minimize water production costs and reduce fuel consumption.

Acknowledgement

This work was supported by Argumentation theory and its application in e-commerce (No. 07JA630052); Research and construction of teaching management policies and systems conducive to the growth of innovative talents (No. Yujiao11847); Innovation of the trinity system of Ideological and political work in Colleges and departments at the grassroots level (No. 042); Research on the relationship between discipline and specialty structure adjustment and economic structure adjustment of colleges and universities in Henan Province (No. Yujiao06346); Research and practice on the construction of campus culture and academic atmosphere conducive to the growth of innovative talents (No. Yujiao06665).

Symbols

A	—	Heat transfer area, m ²
A_d	—	Specific heat transfer area, m ² /m ³
A_{ref}	—	Reference membrane water permeability, kg/m ² /s/pa
B	—	Membrane solute permeability, kg/m ² /s
B_i	—	Exiting brine form i th effect, kg/s
BPE	—	Boiling point elevation, °C
c	—	Concentration, ppm
\dot{C}	—	Annual cost rate, \$/y
CC	—	Capital cost, \$
C_p	—	Specific heat capacity, kJ/kg °C
CRF	—	Capital recovery factor
D_i	—	Produced vapor in i th effect, kg/s
D_r	—	Entrained vapor in last effect, kg/s
D_i'	—	Produced vapor in i th flash box
f_i	—	Inflation rate
GOR	—	Gain output ratio
h	—	Enthalpy, kJ/kg
h_d	—	Heating steam enthalpy, kJ/kg
i	—	Real interest rate
j	—	Nominal interest rate
J_s	—	Salts mass flux through the membrane, kg/m ² /s
J_w	—	Permeate mass flux through the membrane, kg/m ² /s
LCOE	—	Levelized cost of electricity, \$/kWh
LCOW	—	Levelized cost of water, \$/m ³
\dot{m}_{bd}	—	Blowdown mass flow rate, kg/s
M_d	—	Total produced water, kg/s
M_f	—	Feed water mass flow rate, kg/s
\dot{m}_{gas}	—	The mass flow rate of exhaust gas, kg/s
NEA	—	Non-equilibrium allowance, °C
OFC	—	Operating flow cost, \$
PCOE	—	Prime cost of electricity, \$/kWh
PCOW	—	Prime cost of water, \$/m ³
p_d	—	Heating steam pressure, kpa
p_n	—	Entrained vapor pressure, kpa
POE	—	Price of electricity, \$/kWh
POW	—	Price of water, \$/m ³

p_s	—	Motive steam pressure, kpa
Q_d	—	Specific heat consumption, kW/m ³
r	—	RO recovery rate
Rs	—	Salt rejection
s	—	Entropy

Subscripts and superscripts

Abs	—	Absorber
ch	—	Chemical
CI	—	Capital investment
Com	—	Compressor
Con	—	Condenser
CV	—	Control volume
D	—	Destruction
EV	—	Expansion valve
eva	—	Evaporator
ex	—	Exergy
F	—	Fuel
Gen	—	Generator
Gen	—	Generation
HE	—	Heat exchanger
in	—	Inlet
is	—	Isentropic
k	—	k th component
L	—	Loss
LMTD	—	0
Mix	—	Mixer
Ph	—	Physical
pum	—	Pump
pp	—	Pinch point
q	—	Heat transfer
sep	—	Separator
SHE	—	Steam heat exchanger
sys	—	System
th	—	Thermal
tot	—	Total
tur	—	Turbine
W	—	Work
1, 2, ...	—	Cycle locations
0	—	Dead state

Greek symbols

η	—	Efficiency, %
Δp_f	—	Pressure drop along membrane channel, kPa
Δp	—	Transmembrane pressure drop, kPa
ρ	—	Density, kg/m ³
$\Delta \pi$	—	Osmotic pressure difference, kPa
λ	—	Latent heat of evaporation, kJ/kg
ω	—	Entrainment ratio

References

- [1] C.-H. Qi, H.-J. Feng, Q.-C. Lv, Y.-L. Xing, N. Li, Performance study of a pilot-scale low-temperature multi-effect desalination plant, *Appl. Energy*, 135 (2014) 415–422.
- [2] N. Ghaffour, J. Bundschuh, H. Mahmoudi, M.F.A. Goosen, Renewable energy-driven desalination technologies: a comprehensive review on challenges and potential applications of integrated systems, *Desalination*, 356 (2015) 94–114.
- [3] A. Al-Karaghoul, L.L. Kazmerski, Energy consumption and water production cost of conventional and renewable-energy-powered desalination processes, *Renewable Sustainable Energy Rev.*, 24 (2013) 343–356.
- [4] D. Brogioli, F. La Mantia, N.Y. Yip, Thermodynamic analysis and energy efficiency of thermal desalination processes, *Desalination*, 428 (2018) 29–39.
- [5] I.S. Al-Mutaz, I. Wazeer, Comparative performance evaluation of conventional multi-effect evaporation desalination processes, *Appl. Therm. Eng.*, 73 (2014) 1194–1203.
- [6] M. Al-Sahali, H. Ettouney, Developments in thermal desalination processes: design, energy, and costing aspects, *Desalination*, 214 (2007) 227–240.
- [7] A. Al-Karaghoul, D. Renne, L.L. Kazmerski, Technical and economic assessment of photovoltaic-driven desalination systems, *Renewable Energy*, 35 (2010) 323–328.
- [8] A. Alkai, R. Mossad, A. Sharifian-Barforoush, A review of the water desalination systems integrated with renewable energy, *Energy Procedia*, 110 (2017) 268–274.
- [9] M.W. Shahzad, M. Burhan, L. Ang, K.C. Ng, Energy-water-environment nexus underpinning future desalination sustainability, *Desalination*, 413 (2017) 52–64.
- [10] K.C. Ng, M.W. Shahzad, H.S. Son, O.A. Hamed, An exergy approach to efficiency evaluation of desalination, *Appl. Phys. Lett.*, 110 (2017) 184101, <https://doi.org/10.1063/1.4982628>.
- [11] M.W. Shahzad, M. Burhan, H.S. Son, S.J. Oh, K.C. Ng, Desalination processes evaluation at common platform: a universal performance ratio (UPR) method, *Appl. Therm. Eng.*, 134 (2018) 62–67.
- [12] M.W. Shahzad, M. Burhan, K.C. Ng, Pushing desalination recovery to the maximum limit: membrane and thermal processes integration, *Desalination*, 416 (2017) 54–64.
- [13] K.C. Ng, K. Thu, S.J. Oh, L. Ang, M.W. Shahzad, A. Bin Ismail, Recent developments in thermally-driven seawater desalination: Energy efficiency improvement by hybridization of the MED and AD cycles, *Desalination*, 356 (2015) 255–270.
- [14] M.W. Shahzad, K.C. Ng, K. Thu, B.B. Saha, W.G. Chun, Multi effect desalination and adsorption desalination (MEDAD): a hybrid desalination method, *Appl. Therm. Eng.*, 72 (2014) 289–297.
- [15] M.W. Shahzad, K. Thu, Y.-D. Kim, K.C. Ng, An experimental investigation on MEDAD hybrid desalination cycle, *Appl. Energy*, 148 (2015) 273–281.
- [16] M.H. Sharqawy, J.H. Lienhard V, S.M. Zubair, On exergy calculations of seawater with applications in desalination systems, *Int. J. Therm. Sci.*, 50 (2011) 187–196.
- [17] N. Kahraman, Y.A. Cengel, Exergy analysis of a MSF distillation plant, *Energy Convers. Manage.*, 46 (2005) 2625–2636.
- [18] B. Han, Z.L. Liu, H.Q. Wu, Y.X. Li, Experimental study on a new method for improving the performance of thermal vapor compressors for multi-effect distillation desalination systems, *Desalination*, 344 (2014) 391–395.
- [19] H. Sayyaadi, A. Saffari, Thermoeconomic optimization of multi effect distillation desalination systems, *Appl. Energy*, 87 (2010) 1122–1133.
- [20] M.A. Sharaf, A.S. Nafey, L. García-Rodríguez, Exergy and thermo-economic analyses of a combined solar organic cycle with multi effect distillation (MED) desalination process, *Desalination*, 272 (2011) 135–147.
- [21] I.J. Esfahani, A. Ataei, K.V. Shetty, T.S. Oh, J.H. Park, C.K. Yoo, Modeling and genetic algorithm-based multi-objective optimization of the MED-TVC desalination system, *Desalination*, 292 (2012) 87–104.
- [22] S. Sadri, M. Ameri, R.H. Khoshkhou, Multi-objective optimization of MED-TVC-RO hybrid desalination system based on the irreversibility concept, *Desalination*, 402 (2017) 97–108.
- [23] B.A. Qureshi, S.M. Zubair, Exergetic efficiency of NF, RO and EDR desalination plants, *Desalination*, 378 (2016) 92–99.
- [24] C.-J. Lee, Y.-S. Chen, G.-B. Wang, A Dynamic Simulation Model of Reverse Osmosis Desalination Systems, 5th International Symposium on Design, Operation and Control of Chemical Processes, PSE ASIA, Singapore, 2010.

- [25] R.S. El-Emam, I. Dincer, Thermodynamic and thermoeconomic analyses of seawater reverse osmosis desalination plant with energy recovery, *Energy*, 64 (2014) 154–163.
- [26] B. Ortega-Delgado, L. García-Rodríguez, D.-C. Alarcón-Padilla, Thermoeconomic comparison of integrating seawater desalination processes in a concentrating solar power plant of 5 MWe, *Desalination*, 392 (2016) 102–117.
- [27] B. Ortega-Delgado, F. Giacalone, P. Catrini, A. Cipollina, A. Piacentino, A. Tamburini, G. Micale, Reverse electrodialysis heat engine with multi-effect distillation: exergy analysis and perspectives, *Energy Convers. Manage.*, 194 (2019) 140–159.
- [28] S.E. Shakib, M. Amidpour, A. Esmaili, M. Boghrati, M.M. Ghafurian, Various approaches to thermodynamic optimization of a hybrid multi-effect evaporation with thermal vapour compression and reverse osmosis desalination system integrated to a gas turbine power plant, *Int. J. Eng. Trans. B*, 32 (2019) 777–789.
- [29] Y.Q. Wang, N. Lior, Performance analysis of combined humidified gas turbine power generation and multi-effect thermal vapor compression desalination systems—Part 1: the desalination unit and its combination with a steam-injected gas turbine power system, *Desalination*, 196 (2006) 84–104.
- [30] Y.-Y. Lu, Y.-D. Hu, X.-L. Zhang, L.-Y. Wu, Q.-Z. Liu, Optimum design of reverse osmosis system under different feed concentration and product specification, *J. Membr. Sci.*, 287 (2007) 219–229.
- [31] F. Hamrang, A. Shokri, S.M.S. Mahmoudi, B. Ehghaghi, M.A. Rosen, Performance analysis of a new electricity and freshwater production system based on an integrated gasification combined cycle and multi-effect desalination, *Sustainability*, 12 (2020) 7996, doi: 10.3390/su12197996.
- [32] A.O. Bin Amer, Development and optimization of ME-TVC desalination system, *Desalination*, 249 (2009) 1315–1331.
- [33] S.E. Shakib, M. Amidpour, C. Aghanajafi, Simulation and optimization of multi effect desalination coupled to a gas turbine plant with HRSG consideration, *Desalination*, 285 (2012) 366–376.
- [34] H.T. El-Dessouky, H.M. Ettouney, *Fundamentals of salt water desalination*, Elsevier, Hamilton, Ont., 2002.
- [35] F. Vince, F. Marechal, E. Aoustin, P. Bréant, Multi-objective optimization of RO desalination plants, *Desalination*, 222 (2008) 96–118.
- [36] M.H. Khoshgoftar Manesh, H. Ghalami, M. Amidpour, M.H. Hamed, Optimal coupling of site utility steam network with MED-RO desalination through total site analysis and exergoeconomic optimization, *Desalination*, 316 (2013) 42–52.
- [37] M. Meratizaman, S. Monadizadeh, M. Amidpour, Introduction of an efficient small-scale freshwater-power generation cycle (SOFC–GT–MED), simulation, parametric study and economic assessment, *Desalination*, 351 (2014) 43–58.
- [38] F. Masoumi, S. Najjar-Ghabel, A. Safarzadeh, B. Sadaghat, Automatic calibration of the groundwater simulation model with high parameter dimensionality using sequential uncertainty fitting approach, *Water Supply*, 20 (2020) 3487–3501.
- [39] Q.H. Bai, Analysis of particle swarm optimization algorithm, *Comput. Inf. Sci.*, 3(2010) 180, doi: 10.5539/cis.v3n1p180.